2014

Galaxy Zoo: CANDELS Barred Disks and Bar Fractions

Karen Masters
Haverford College, klmasters@haverford.edu

Brooke D. Simmons

Thomas Melvin

Chris Lintott

Repository Citation

Galaxy Zoo: CANDELS barred discs and bar fractions[★]

B. D. Simmons,[1][†] Thomas Melvin,[2] Chris Lintott,[1,3] Karen L. Masters,[2,4]
Kyle W. Willett,[5] William C. Keel,[6] R. J. Smethurst,[1] Edmond Cheung,[7]
Robert C. Nichol,[2,4] Kevin Schawinski,[8] Michael Rutkowski,[5] Jeyhan S. Kartaltepe,[9][‡]
Eric F. Bell,[10] Kevin R. V. Casteels,[11] Christopher J. Conselice,[12] Omar Almaini,[12]
Henry C. Ferguson,[13] Lucy Fortson,[5] William Hartley,[8,12] Dale Kocevski,[14]
Anton M. Koekemoer,[13] Daniel H. McIntosh,[15] Alice Mortlock,[12]
Jeffrey A. Newman,[16] Jamie Ownsworth,[12] Steven Bamford,[12] Tomas Dahlen,[13] Sandra
M. Faber,[17] Steven L. Finkelstein,[18] Adriano Fontana,[19] Audrey Galametz,[19] N.
A. Grogin,[13] Ruth Grützbauch,[12,20] Yicheng Guo,[17] Boris Häußler,[1,12,21]
Kian J. Jek,[§] Sugata Kaviraj,[21] Ray A. Lucas,[13] Michael Peth,[22] Mara Salvato,[23]
Tommy Wiklind[24] and Stijn Wuyts[23]

Affiliations are listed at the end of the paper

ABSTRACT

The formation of bars in disc galaxies is a tracer of the dynamical maturity of the population. Previous studies have found that the incidence of bars in discs decreases from the local Universe to $z \sim 1$, and by $z > 1$ simulations predict that bar features in dynamically mature discs should be extremely rare. Here, we report the discovery of strong barred structures in massive disc galaxies at $z \sim 1.5$ in deep rest-frame optical images from the Cosmic Assembly Near-Infrared Deep Extragalactic Legacy Survey. From within a sample of 876 disc galaxies identified by visual classification in Galaxy Zoo, we identify 123 barred galaxies. Selecting a subsample within the same region of the evolving galaxy luminosity function (brighter than L^*), we find that the bar fraction across the redshift range $0.5 \leq z \leq 2$ ($f_{\rm bar} = 10.7^{+6.3}_{-3.5}$ per cent after correcting for incompleteness) does not significantly evolve. We discuss the implications of this discovery in the context of existing simulations and our current understanding of the way disc galaxies have evolved over the last 11 billion years.

Key words: galaxies: evolution – galaxies: general – galaxies: spiral – galaxies: structure.

1 INTRODUCTION

Large-scale galactic stellar bars are thought to form within dynamically cold, rotationally supported discs (Athanassoula 2005; Combes 2009; Athanassoula, Machado & Rodionov 2013; Sellwood 2013). Thus, the evolution of the fraction of disc galaxies with bar features traces the overall evolution of disc galaxy dynamics. Locally, bars are present in $\sim$25–50 per cent of disc galaxies (where bars are classified either visually, from Fourier analysis, or from examining elliptical isophotes; e.g. Odewahn 1996; Elmegreen, Elmegreen & Hirst 2004b; Aguerri, Mndez-Abreu & Corsini 2009; Nair & Abraham 2010; Masters et al. 2011; Cheung et al. 2013), with their abundance steadily decreasing to $\sim$10 per cent of disc galaxies at $z \sim 1$ (Abraham et al. 1999; Sheth et al. 2003; Elmegreen et al. 2004b; Elmegreen & Elmegreen 2005; Sheth et al. 2008; Melvin et al. 2014).

The lower incidence of bars at higher redshifts may be in part be due to the increased incidence of mergers and galaxy interactions (Conselice et al. 2003; Lotz et al. 2011; Casteels et al. 2013), which disrupt and heat discs, destroying or preventing the formation of bars. More generally, disc galaxies at $z \sim 1$ tend to be less dynamically 'settled' than their more local counterparts, with

a lower rotation velocity compared to velocity dispersion as redshift increases (Förster Schreiber et al. 2011; Kassin et al. 2012). The redshift dependence of bar fractions may also be related to the expected increase in disc gas fraction with redshift; this has been observed directly via the increased M_{gas}/M_{star} from CO observations (e.g. Tacconi et al. 2010, 2013, for a detailed review, see Carilli & Walter 2013). The presence of a bar in a galaxy is anticorrelated with specific star formation rate (Cheung et al. 2013) and disc gas fraction (Masters et al. 2012), in agreement with theoretical predictions (Friedli & Benz 1993; Berentzen et al. 2007; Villa-Vargas, Shlosman & Heller 2010; Athanassoula et al. 2013), although a high gas fraction does not entirely preclude the existence of a bar (Nair & Abraham 2010; Masters et al. 2012).

The current theoretical understanding of bar fraction evolution suggests that disc galaxies at $z > 1$ may be too dynamically hot to form bars: Kraljic, Bournaud & Martig (2012) find no observable bars within a simulated sample of galaxies at $z \sim 1.5$. However, other simulations explore the impact of tidal heating and galaxy harassment, which can either inhibit bar formation *or* promote it, depending on mass (Noguchi 1988; Moore et al. 1996; Skibba et al. 2012). Testing the viability of the proposed mechanisms responsible for the redshift dependence of bar fractions requires high-resolution imaging over a large area of the sky to observe statistically significant samples in multiple redshift bins and adequate spatial resolution to resolve galactic-scale bars in the rest-frame optical (since the detectability of bars decreases rapidly bluewards of the 4000 Å break; Sheth et al. 2008).

These observing requirements currently limit studies of disc populations via bar fractions to surveys with the *Hubble Space Telescope (HST)*. Previous studies have used the optical cameras on *HST* to examine bar fractions to $z \sim 1$. In this paper, we present the first results from Galaxy Zoo morphological classifications of galaxies imaged by the Cosmic Assembly Near-Infrared Deep Extragalactic Legacy Survey (CANDELS; Grogin et al. 2011; Koekemoer et al. 2011), which uses *HST's* near-infrared Wide-Field Camera 3 (WFC3) and which allows us to probe the bar fractions of galaxies with $L > L^*$ out to $z \sim 2$.

In Section 2, we describe our sample selection, including a summary of Galaxy Zoo classifications of CANDELS galaxies and how discs and bars are selected. We also explore any potential biases that may affect our results. We present our results in Section 3, with a discussion including comparison to simulated predictions in Section 4, and a summary in Section 5. Throughout this paper, we use the AB magnitude system, and where necessary we adopt a cosmology consistent with Λ cold dark matter, with $H_0 = 70 \, \mathrm{km \, s^{-1} \, Mpc^{-1}}$, $\Omega_m = 0.3$, and $\Omega_\Lambda = 0.7$ (Bennett et al. 2013).

2 DATA

2.1 CANDELS

The Cosmic Assembly Near-infrared Extragalactic Legacy Survey (CANDELS; Grogin et al. 2011; Koekemoer et al. 2011) is an *HST* Treasury programme combining optical and near-infrared imaging from the Advanced Camera for Surveys (ACS) and Wide Field Camera (infrared channel; WFC3/IR) across five well-studied survey fields (GOODS-North and -South, Giavalisco et al. 2004; EGS, Davis et al. 2007; UDS, Cirasuolo et al. 2007; Lawrence et al. 2007; and COSMOS, Scoville et al. 2007) using a two-tiered 'deep' and 'wide' approach. Each of the wide fields (UDS, COSMOS, EGS, and flanking fields to the GOODS-S and GOODS-N deep fields) are imaged over two orbits in WFC3/IR, split in a 2:1 ratio between

filters *F*160*W* and *F*125*W*, respectively, with parallel exposures in *F*606*W* and *F*814*W* using ACS. Each of the deep fields (GOODS-S and GOODS-N) are imaged over at least four orbits each in both the *F*160*W* and *F*125*W* filters and three orbits in the *F*105*W* filter, with ACS exposures in *F*606*W* and *F*814*W* in parallel. These are reduced and combined to produce a single mosaic for each field in each band, with drizzled resolutions of 0.03 and 0.06 arcsec per pixel for ACS and WFC3/IR, respectively (a process described in detail by Koekemoer et al. 2011).

Here, we use the CANDELS ACS and WFC3/IR images from within the COSMOS, GOODS-South, and UDS fields for which raw classifications from the Galaxy Zoo project are presently available. The WFC3/IR observations of these fields cover approximately 0.15 deg^2 combined. The Galaxy Zoo classifications are based on colour images created using the Lupton et al. (2004) asinh stretch method with resolution-matched WFC3 *F*160*W*, *F*125*W*, and ACS *F*814*W* as red, green, and blue channels, respectively. Some of the colour images use ACS data that were observed during previous surveys (Giavalisco et al. 2004; Davis et al. 2007; Koekemoer et al. 2007; Scoville et al. 2007) and re-analysed by the CANDELS pipeline.

2.2 Classifications

Galaxy Zoo provides quantified visual morphologies by obtaining multiple independent classifications for each galaxy. Beginning in 2007, more than 1000 000 galaxy images in total from the Sloan Digital Sky Survey and the *HST* have each been classified by typically ∼40 independent volunteers via a web interface.[1] The initial version of the project (Lintott et al. 2008, 2011) asked a single question per galaxy (whether the galaxy was spiral or elliptical). Subsequent versions have collected more detailed morphological information, including finer substructures of disc galaxies such as bulge strength and bars, via a tiered classification tree (e.g. Willett et al. 2013; Melvin et al. 2014). All previous Galaxy Zoo projects have incorporated extensive analysis of volunteer classifications to measure classification accuracy and bias and compute user weightings (for a detailed description of debiasing and consistency-based user weighting, see section 3 of Willett et al. 2013). The classifications are highly accurate and the high number of independent classifications per galaxy has enabled a diverse range of investigations in the overall field of galaxy evolution (e.g. Darg et al. 2010a,b; Masters et al. 2011; Skibba et al. 2012; Casteels et al. 2013).

This work uses classifications collected during the fourth release of Galaxy Zoo, specifically of 49 555 images from the COSMOS, GOODS-South, and UDS fields in the CANDELS survey (hereafter GZ-CANDELS). The data set was initially composed of all sources having *F*160*W* (*H*) apparent magnitude <25.5. This limit is considerably brighter than the expected 5σ extended-source detection limits reported in Grogin et al. (2011). Within this sample, 58 per cent of sources have $25.5 < H < 24.5$, and 31 per cent of sources have $H < 23.5$. (We note that this brighter subsample includes 95 per cent of galaxies later selected as 'featured' galaxies, Section 2.4).

Several months after the launch of GZ-CANDELS, an initial analysis motivated by community[2] tags of sources considered too faint to classify resulted in the application of systematic cuts in magnitude-surface-brightness space and the early retirement of 1555 point-like

---

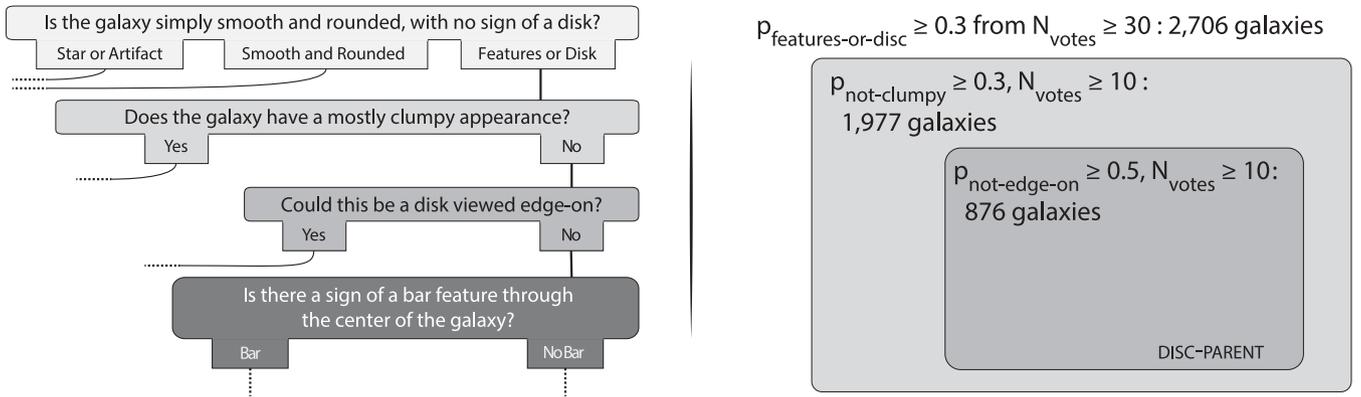[1] zoo4.galaxyzoo.org

[2] talk.galaxyzoo.org

Figure 1. Left: partial Galaxy Zoo: CANDELS classification tree, starting with the first question (top) and leading to the bar feature question. There are 17 questions total in the tree; the bar question is a fourth-tier task. Right: selection of the featured, not-edge-on disc galaxy sample (876 galaxies, hereafter called the DISC-PARENT sample) in GZ-CANDELS; relative box areas are scaled to the sample sizes. This selection was made independently of restrictions on redshift or luminosity (a full description of the sample selection is given in Section 2.4). Eight independent classifiers subsequently examined each of the 876 DISC-PARENT galaxies for evidence of a bar.

sources and 11 837 faint, low-surface-brightness galaxies without resolvable fine features. Although the project is still ongoing, as of the date of this analysis each of the remaining objects has received at least 40 independent classifications (mean number 43, maximum 81). For each source classified by volunteers in GZ-CANDELS, all independent classifications are combined to produce 'vote percentages', where a vote percentage p for a given answer to a given question in the classification tree is the number of votes for that answer divided by the number of classifiers who answered the question.

The classification tree used for GZ-CANDELS (Simmons et al., in preparation, see Fig. 1 for the portion relevant here) first asks volunteers to choose whether a galaxy is mostly smooth, has features, or is a star/artefact. The bar classification question ('Is there a sign of a bar feature through the center of the galaxy?') is reached once a volunteer has chosen 'Features or Disk' as an answer to the first question and has subsequently said the galaxy does *not* have a mostly clumpy appearance, nor is it an edge-on disc. The bar classification is therefore a fourth-tier task, and the number of volunteers per galaxy who answer the bar question varies depending on responses to the earlier tasks. We discuss the details of the disc and barred disc galaxy sample selections based on the tiered questions in the tree in Section 2.4.

We note that an independent effort is underway to collect at least three visual classifications per galaxy from CANDELS team members (classifications for one field have been published; Kartaltepe et al. 2014). These classifications use a different approach to the decision tree method used by Galaxy Zoo; we defer a full analysis between these classifications and Galaxy Zoo results to our upcoming data release paper.

2.3 Redshifts

Each of the fields covered by CANDELS data has considerable ancillary data from previous and ongoing work. In addition to newly calculated photometric redshifts in CANDELS (based on a Bayesian approach combining results from multiple different analyses; Dahlen et al. 2013), we assemble additional photometric and spectroscopic redshifts from the available literature. For galaxies in the COSMOS field, we combine spectroscopic redshifts from the zCOSMOS project (Lilly et al. 2007) with photometric redshifts from COSMOS (Ilbert et al. 2009) and from the NEWFIRM medium-band survey (Whitaker et al. 2011). In the GOODS-South

field, we use the catalogue of Cardamone et al. (2010), who added photometric redshifts based on deep broad- and medium-band data from MuSYC (Gawiser et al. 2006) to available spectroscopic redshifts compiled from multiple sources (Cimatti et al. 2002; Le Fèvre et al. 2004; Vanzella et al. 2008; Balestra et al. 2010). In the UDS field, we use available spectroscopic (Simpson et al. 2012) and photometric redshifts (Hartley et al. 2013), the latter of which make use of deep multiwavelength coverage from the UKIRT Infrared Deep Sky Survey (UKIDSS) as well as J- and H-band magnitudes from CANDELS. Of the 49 555 galaxies originally included in Galaxy Zoo: CANDELS, 46 234 currently have spectroscopic (2886) or photometric (43 348) redshifts. Where available, agreement between spectroscopic and photometric redshift is generally very good, with $\Delta z \equiv \sigma_z / (1 + z_{\mathrm{spec}}) = 0.02$ and ~ 8 per cent of sources having $\Delta z > 0.2$. The use of photometric redshifts introduces an uncertainty of less than 1 per cent into the population bar fractions discussed in Section 3. These uncertainties are discussed along with other possible sources of error in Section 2.5.

2.4 Sample selection

A full reduction of the GZ-CANDELS classifications, resulting in a catalogue of morphological measurements that incorporates weighted user votes and adjustments for biases in classifications due to cosmological dimming and resolution effects for each galaxy, is ongoing. Here, we use the raw vote percentages, which have been neither weighted nor debiased. The effects of using raw versus the reduced classifications are twofold. First, the unweighted votes are likely biased in the first question towards an excess of votes for 'Star or Artifact' (see Willett et al. 2013 for a discussion of how inconsistent votes are downweighted in Galaxy Zoo 2, which has a similar classification tree). Secondly, the effects of surface-brightness dimming and loss of spatial resolution are not accounted for in the vote percentages, which is potentially a significant effect in a sample extending to $z \sim 2$ in the rest-frame optical. We minimize the effect of surface-brightness dimming via luminosity cuts described in Section 2.4.1, and address the lack of user weighting via threshold cuts in classification vote fractions, as described below.

To favour completeness in the final disc galaxy sample and to minimize the impact of the lack of user weighting, we employ a lower vote percentage threshold when selecting 'featured' galaxies than is typical when using weighted data. We select as 'featured'
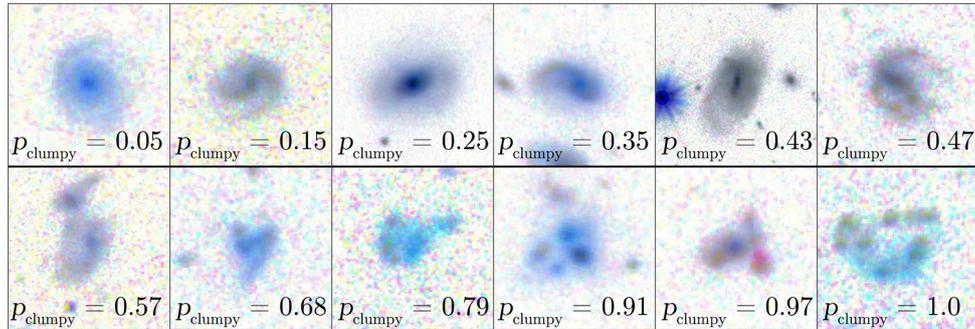
Figure 2. Examples of galaxies in GZ-CANDELS with different vote percentages for the question 'Does the galaxy have a mostly clumpy appearance?' Each galaxy is labelled with its clumpy vote percentage, where p_{clumpy} indicates the fraction of classifiers who answered 'Yes' to the question. (For comparison to the selection described in Section 2.4 and Fig. 1, note that $p_{not-clumpy} = 1 - p_{clumpy}$.) In order to favour inclusiveness of clumpy discs while ensuring enough votes for the subsequent questions along the not-clumpy branch of the classification tree, all galaxies with $p_{clumpy} < 0.7$ are included in the disc sample if they also meet the other selection criteria described in Section 2.4.

galaxies those where at least 30 per cent of votes (out of at least 30 volunteers total) were registered for 'Features or Disk'. This selects 2706 featured galaxies. For comparison, a more typical threshold for weighted classifications is $p_{features-or-disc} = 0.5$ (e.g. Melvin et al. 2014). After the first question, the user weighting used by previous Galaxy Zoo data reductions (Lintott et al. 2008; Bamford et al. 2009; Willett et al. 2013) affects vote percentages by typically no more than a few per cent. We therefore expect the lack of weighting to have little to no systematic effect on additional vote percentages.

Subsequent to the featured galaxy selection, we select a subsample where at least 30 per cent of volunteers (where a minimum of 10 answered the question) registered a vote for 'no' to the question 'Does the galaxy have a mostly clumpy appearance?' Fig. 2 shows examples of galaxies along the full range of clumpy/not-clumpy vote percentages. We include the clumpy selection in order to explicitly consider each branch of the classification tree that leads to the bar-feature question, but the threshold is deliberately lower than previous studies (Melvin et al. 2014) to favour inclusiveness of clump-dominated discs that may be more prevalent at higher redshift (e.g. Elmegreen, Elmegreen & Hirst 2004a; Elmegreen & Elmegreen 2005; Elmegreen et al. 2007; Förster Schreiber et al. 2011) while removing galaxies with no apparent underlying discs or whose morphologies preclude evaluation of potential bar features. This selection removes 729 sources in total, leaving 1977 galaxies. However, were we to ignore the clump-threshold criterion completely, this would only affect the final sample of disc galaxies at the 1 per cent level, due to the subsequent inclination and luminosity selection criteria. Our qualitative results are thus not sensitive to the specific choice of clumpy threshold within the range $0.1 \leq p_{not-clumpy} \leq 0.6$.

We also require that 50 per cent of volunteers (of at least 10) registered a vote for a disc galaxy that is 'not-edge-on'. This is a deliberately conservative choice to reflect the fact that bars would be invisible in edge on systems (the thresholds used to select disc features are less strict to favour completeness).[3] This selects a sample of 876 disc galaxies, within each of which a bar may be identified, if it exists. This parent sample of 876 not-edge-on disc galaxies is referred to hereafter as the DISC-PARENT sample. As a sanity check on the selection of discs, we examine the Sérsic (1968) indices of the DISC-PARENT sample using the parametric fits of van der Wel

et al. (2012). We find that the distribution of Sérsic indices is peaked at $n = 1.4$, with $\sigma_n = 0.6$, fully consistent with a disc-dominated sample (e.g. Häussler et al. 2007; Simmons & Urry 2008).

Fig. 1 shows a visual representation of this sample selection, from which a further subsample of barred galaxies may be identified. However, approximately 20 per cent of these 876 galaxies received less than 10 raw votes *total* for the question 'Is there any sign of a bar feature through the center of the galaxy?', a consequence of the broad initial selection of featured galaxies and the multiply branched nature of the classification tree. Because of this incompleteness and the lower number of votes per galaxy in the fourth tier of the classification tree (the position of the bar question), within the DISC-PARENT sample the raw bar fractional vote is statistically useful, but uncertain for individual galaxies.

We therefore elected to supplement the volunteer data with visual classifications from the Galaxy Zoo science team to select the subsample of barred disc galaxies. Eight of the authors[4] inspected each of the 876 DISC-PARENT galaxies for evidence of a bar. These votes were unanimous approximately 60 per cent of the time, either for a bar feature (23 galaxies) or no bar (512 galaxies). Among galaxies where the science team voted unanimously that a bar is present, the median volunteer bar vote percentage and interquartile range are $0.6^{+0.17}_{-0.06}$. Among galaxies where the science team was unanimous that a bar is *not* present, the median volunteer bar vote percentage and interquartile range are $0.1^{+0.08}_{-0.1}$. The science team and volunteer bar vote percentages correlate ($r = 0.8$ with very high significance:[5] p-value $\rightarrow 0$), although the low number of volunteer votes for many objects means the dispersion in the correlation is high. We therefore choose not to include the incomplete volunteer votes for this question, considering only the science-team classifications in the determination of the bar percentage, $p_{s,bar}$. Following vote percentage thresholds used in previous studies, we mark a galaxy as barred if at least half of the science-team classifiers indicated the presence of a bar ($p_{s,bar} \geq 0.5$). This vote fraction threshold has been shown to select strong bars (Masters et al. 2011; Willett et al. 2013; Melvin et al. 2014). Using this vote percentage threshold identifies 123 barred disc galaxies (hereafter the BAR-PARENT sample) from among the DISC-PARENT sample of 876 disc galaxies selected from the full GZ-CANDELS sample.

---

[3] The discussion in Section 3 assumes that the bar fraction is the same in edge-on galaxies as face-on galaxies; an application of the results to include strongly clump-dominated galaxies requires a similar assumption.

[4] BDS, TM, KWW, WCK, MR, KLM, RJS, EC.

[5] The statistics package R reported $p < 2.2 \times 10^{-16}$, which indicates a value smaller than can be precisely reported using floating-point precision.

2.4.1 Redshift and luminosity selections

The absolute *H*-band magnitudes in the sample are plotted as a function of redshift in Fig. 4. Within the DISC-PARENT sample, 525 galaxies have redshifts between $0.5 \leq z \leq 2.0$; within the BAR-PARENT sample, 61 galaxies have $0.5 \leq z \leq 2.0$. Within this redshift range, all flux measured in the WFC3 *H* band is redwards of the 4000 Å break. Examples of barred and unbarred galaxies are shown in Fig. 3.

To minimize any bias caused by surface-brightness dimming at higher redshifts, we additionally employ a conservative luminosity cut when examining bar fractions, choosing a minimum *H* absolute magnitude of -23.15 at $z = 2$. This ensures that galaxy features can be detected within the subsample at all $z < 2$. We note that this is brighter than the knee of the rest-frame-*V*-band luminosity function at this redshift (Marchesini et al. 2012). In order to examine similar populations across our entire redshift range, we use a redshift-dependent luminosity cut based on selecting the same region of the evolving luminosity function (corrected to observed *H* band; Blanton & Roweis 2007; Marchesini et al. 2012): this selection is shown as a parallelogram shape in Fig. 4. This final cut produces 370 not-edge-on disc galaxies within these luminosity and redshift bounds, of which 56 have strong bar signatures. Hereafter, we refer to these as the DISC-LZ and BAR-LZ samples, respectively. We note that our results are robust to small variations in the redshift and luminosity thresholds chosen for the sample. For example, our qualitative result does not change if we use a fixed luminosity/stellar mass range.

2.4.2 Completeness corrections

For galaxies within the luminosity ranges considered here and observed at the depth of the CANDELS images (even the shallower 'wide' fields), the composition of the final DISC-LZ sample is unlikely to be affected by surface-brightness dimming. Furthermore, the analysis in this paper is concerned with large-scale, strong galactic bars, which are less affected by surface-brightness dimming or the effects of diminishing resolution than weaker features. The result is a conservative selection with respect to feature detection, in the sense that both strong bars in particular and discs with features in general are unlikely to be missed.

However, it is necessary to account for the possibility that a substantial number of rotationally supported discs with deceptively smooth distributions of light (i.e. disc galaxies that are entirely lacking in 'features') might be present in the sample. The presence of such a population would result in our measured bar fractions (Section 3) being overestimates.
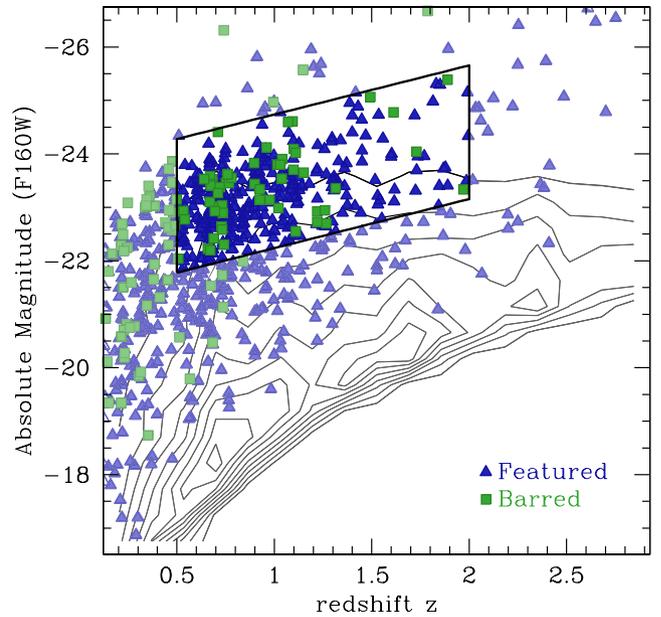

Figure 4. Absolute *H*-band magnitude versus redshift for all sources with $H < 25.5$ (contours in steps of 10 per cent) and 876 discs (DISC-PARENT sample; blue triangles), of which 123 galaxies show clear evidence of a bar (BAR-PARENT sample; green squares). To facilitate comparison between lookback times, avoid biases due to surface-brightness dimming when calculating bar fractions, and ensure all observed *H*-band flux is redwards of the 4000 Å break, we select subsamples within the same region of the evolving galaxy luminosity function (Marchesini et al. 2012) and $0.5 \leq z \leq 2$ (parallelogram). Within this region there are 370 disc galaxies (DISC-LZ sample), 56 of which have clear evidence of bars (BAR-LZ sample).

To estimate the maximum contamination from such a population, we examine 'smooth' galaxies. In particular, we examine a subsample of all galaxies within our luminosity and redshift cuts (Section 2.4.1) with fewer than 30 per cent of votes in the first question (from a total of at least 30) for either 'Features or Disk' or 'Star or Artifact' (hereafter the SMOOTH-LZ sample). We assume that this sample has a mix of rotation-dominated and dispersion-dominated galaxies, and we assess the maximum fraction of this sample that could reasonably be a disc population using measurements of axial ratios for these systems (Galametz et al. 2013; Guo et al. 2013; Fontana et al. 2014; Peth et al., in preparation).

Typical low-redshift disc galaxies have minimum (i.e. edge-on) axial ratios varying from $0.08 \leq (b/a)_{min} \leq 0.2$ (depending on bulge strength; e.g. Padilla & Strauss 2008), and this minimum disc thickness likely increases somewhat for disc galaxies at higher
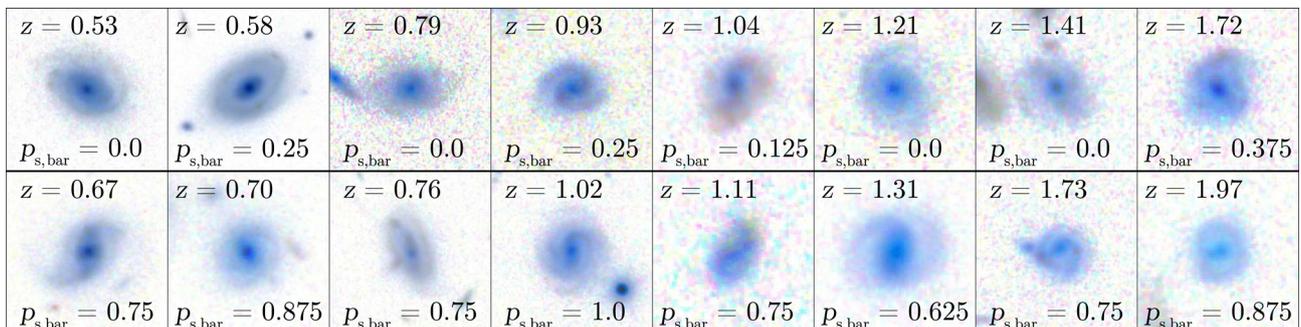

Figure 3. Examples of disc galaxies in GZ-CANDELS whose bar vote percentage ($p_{s, bar}$) places them in the unbarred (top row) and barred (bottom row) subsamples.

redshift (e.g. Förster Schreiber et al. 2009; Law et al. 2009). To account conservatively for the possible thickening of discs, we assume that *all* featureless galaxies with axial ratios $b/a \leq 0.4$ (i.e. ellipticities $\epsilon \geq 0.6$) are disc galaxies. Assuming these are part of a randomly oriented population of discs, we use their expected distribution of axial ratios (Lambas, Maddox & Loveday 1992; Binney & Merrifield 1998; Padilla & Strauss 2008; Law et al. 2012b) to constrain the fraction of the SMOOTH-LZ sample that is composed of this hypothetical disc population. This fraction is ≈19 per cent for the full sample, and generally increases with redshift within our limits between 15 and 25 per cent. It should be noted that this is likely an overestimate of the contamination, as dispersion-dominated early-type galaxies with smooth light profiles and low axial ratios certainly exist (Emsellem et al. 2011).

In order to account for this possible contamination, we then apply these fractions to that part of the SMOOTH-LZ sample that is consistent with the not-edge-on selection described for the DISC-LZ sample above. We add those galaxy counts to each redshift bin of the DISC-LZ sample. The completeness correction effectively increases the size of the DISC-LZ sample to 525 galaxies. The bar fractions derived below are thus conservative lower limits.

2.5 Uncertainties and measurement errors

The goal of this study is to determine the fraction of the $L > L^*$ disc galaxy population at redshifts $0.5 \leq z \leq 2$ with strong bar features. We must therefore account for several potential sources of uncertainty in the measurement of the population bar fraction.

First, there are sampling errors due to the fact that we cannot sample the complete population of disc galaxies. When considering fractions of populations with a given attribute (such as a bar feature), the Normal approximation systematically underestimates proportional confidence errors when the true population fraction approaches 0 or 1, especially for small sample sizes. On the other hand, Cameron (2011) convincingly argues that an alternative and often-used approach estimating wider confidence intervals in the case of small number statistics (Clopper & Pearson 1934; Gehrels 1986) systematically overestimates these confidence intervals. For that reason, Cameron advocates a Bayesian approach to binomial confidence intervals, which we adopt in this study to estimate the uncertainty due to incomplete sampling. The full 68 per cent confidence intervals for bar fractions in this study range from 0.04 to 0.07 around the measured fractions at each redshift. We additionally apply this method to re-calculate uncertainties for all the previous studies of bar population fractions to which we compare our results in Section 3.

There are also numerous sources of standard measurement error that could affect the measured population fractions. Here, we consider the two additional sources of measurement error likely to have the greatest effect on the bar fractions: classification errors and errors in photometric redshifts.

We have estimated the uncertainties introduced into the bar fractions by photometric redshift errors via a bootstrap resampling of the redshifts in the DISC-PARENT sample. Specifically, we resample the DISC-PARENT sample 10^5 times using a Monte Carlo method to vary the redshifts within the measured Δz; 92 per cent of the sample is assumed to vary normally around this value, and 8 per cent are catastrophic outliers with errors uniformly distributed between $0.2 \leq \Delta z \leq 2$. Errors on spectroscopic redshifts are assumed to be negligible. For each resampling, we re-calculate luminosities and re-select the DISC-LZ and BAR-LZ samples based on the re-sampled luminosities and redshifts. Using this method, we find the
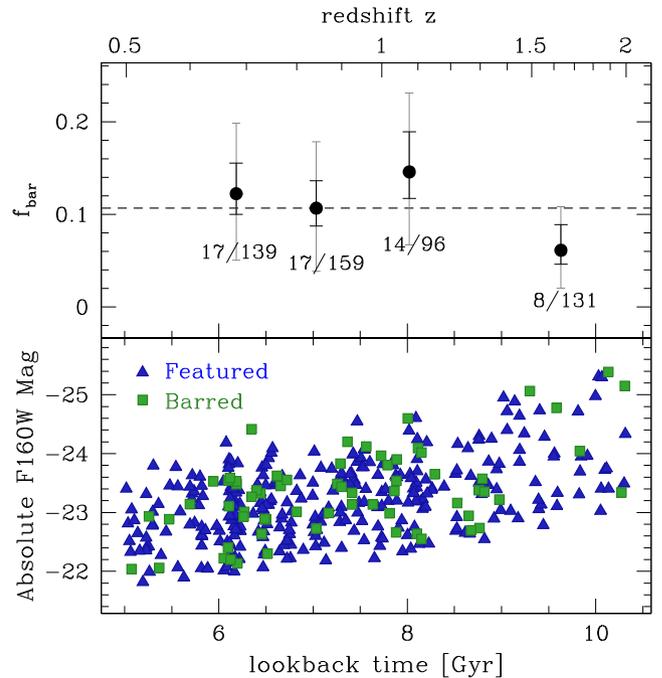

Figure 5. Top panel: bar fraction versus lookback time (black circles) for the completeness-corrected DISC-LZ sample. Black error bars are 68 per cent Bayesian binomial confidence intervals (Cameron 2011); grey error bars are 1σ uncertainties combining the binomial confidence intervals with uncertainties due to photometric redshift measurement error and classification error (described in Section 2.5). Within the uncertainties, the bar fraction is consistent with no evolution from $0.5 \leq z \leq 2$. Bins were chosen to enclose similar lookback time intervals; the bar fraction across all bins ($10.7^{+6.3}_{-3.5}$ per cent, combined errors) is shown as a dashed line. Bottom panel: absolute *H*-band magnitudes of the featured disc sample from which the fractions are drawn.

additional uncertainties introduced into the bar fraction are small: $\sigma_{\mathrm{frac,photoz}} \lesssim 0.01$.

Errors in visual classifications are greatly reduced by the Galaxy Zoo approach, which combines multiple independent classifiers. Each of the galaxies in the DISC-PARENT sample have at least 40 independent classifications, enough that answers given in the first few branches of the classification tree have converged to a stable percentage of votes for a given feature (Willett et al. 2013). The selection method using vote percentages has also been demonstrated in previous studies to be very robust.

However, as described above, the volunteer classifications for the fourth-tier question, which directly asks about bar features (Fig. 1), are not yet complete and have not uniformly converged in the DISC-PARENT sample. The bar classifications from eight of the authors of this study are complete, but the smaller number may introduce additional uncertainties into the measured bar fractions. Specifically, the mean and median of the individually classified population bar fractions are fully consistent with the bar fractions described in Section 3, but the spread from individual classifiers ranges from $\sigma_{\mathrm{frac,\,class}} \approx 0.04$ to 0.07, depending on redshift bin.

Combining the errors from these three sources produces estimates of combined 1σ uncertainties of $0.04 \leq \sigma_{\mathrm{frac,\,comb}} \leq 0.09$, which are shown in Fig. 5. We also show the error bars from the binomial confidence intervals calculated according to Cameron (2011) in both Figs 5 and 6, as these error bars provide a uniform context to compare with the results from other studies.
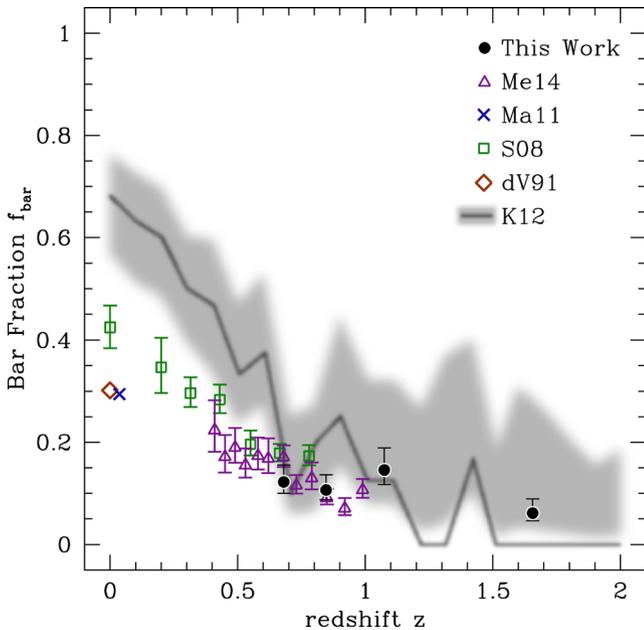
Figure 6. Fraction of disc galaxies having a strong bar feature versus redshift, in the context of other work assessing visual strong bar fraction. All shading and error bars indicate 1σ Bayesian binomial confidence intervals (Cameron 2011); where necessary, we have re-calculated uncertainties of other studies so that all uncertainties shown here are based on the same method. Error bars for the Masters et al. (2011, Ma11, blue cross) and de Vaucouleurs et al. (1991, dV91, red diamond) fractions are smaller than the size of the points and are omitted. At higher redshift, bar fractions in this work (black circles) at $z < 1$ are consistent with those of Sheth et al. (2008, S08, green squares) and Melvin et al. (2014, Me14, purple triangles) despite differences in selection methods and including our conservative completeness correction. Kraljic et al. (2012, K12) computed the fraction of strong bars to $z = 2$ among modelled disc galaxies that evolved to stellar masses $M_* \approx 10^{10-11} M_\odot$ (shaded region); the predicted bar fraction is consistent with that observed here within the uncertainties, although we note that the differences between simulated and observed mass/luminosity ranges make direct quantitative comparisons more difficult.

3 RESULTS: BAR FRACTIONS

The fraction of disc galaxies with visually identified strong bars between $0.5 \leq z \leq 2$ is ~ 10 per cent, a figure that is robust to moderate changes in luminosity ranges or vote fractions for detected features, lack of clumpiness, disc inclination angle, and strong bar features. Fig. 5 shows the bar fraction with lookback time, from $t_{lb} = 5.0$ Gyr ($z = 0.5$) to 10.2 Gyr ($z = 2.0$). The DISC-LZ sample encompasses the same subset of the galaxy luminosity function relative to the evolving L^*. This conservative selection to ensure detectability of features (or lack thereof) to $z = 2$ means the galaxies examined here are all brighter than L^* at their epoch.

Fig. 6 shows the visually identified strong bar fraction versus redshift in the context of other work, both observational and theoretical. Within the redshift range where we overlap with other observational studies, the bar fraction is consistent. However, the bar fraction with redshift appears to flatten at $z > 1$.

Within this sample, and given the uncertainties described in Section 2.5, the bar fraction is consistent with zero evolution between $1 < z < 2$. Many studies of the bar fraction at $z \lesssim 1$ find that the bar fraction does evolve, though these findings are not unanimous (Abraham et al. 1996, 1999; Elmegreen et al. 2004b; Jogee et al.

2004; Elmegreen & Elmegreen 2005; Sheth et al. 2008; Cameron et al. 2010; Melvin et al. 2014). Two independent studies of the full COSMOS-ACS sample (Sheth et al. 2008; Melvin et al. 2014) show that the fraction of visually identified strong bars decreases with redshift, from approximately 35 per cent at $z = 0.2$ to 15 per cent at $z = 1$.

Using zoom-in cosmological simulations of 33 field and loose group galaxies, Kraljic et al. (2012) find that disc galaxies at $z \gtrsim 1$ are generally too dynamically hot to become unstable to bar formation; this manifests itself as a decreasing bar fraction with increasing redshift. Although the quantitative bar fractions in their simulations depend on the threshold used to define a bar feature, the fraction of disc galaxies hosting bars drops to zero, or near zero, by any definition they use (Fig. 6 shows their standard 'strong bar' definition, which is the closest to observational samples defined by visual classifications such as those here and in previous work; Masters et al. 2011; Willett et al. 2013; Melvin et al. 2014). This initially appears inconsistent with our results showing a low, but non-zero, bar fraction (the observed bar fraction is formally inconsistent with 0 at the $>3\sigma$ level). However, due to the very small number of simulated galaxies in Kraljic et al. that are disc galaxies at $z > 1$, a complete lack of bar feature detection within the subset of their sample identified as disc galaxies does not directly predict a 0 per cent bar fraction, and given the small sample the uncertainties quoted in that study (using the Normal approximation) are likely underestimates. We have re-calculated the uncertainties quoted in Kraljic et al., using the Bayesian approach to compute binomial confidence intervals (Cameron 2011) discussed in Section 2.5. Given this approach, the lack of detection of bars at $z > 1.5$ in the simulations is consistent with a bar fraction of up to ≈ 30 per cent at these redshifts, within the recalculated 68 per cent confidence intervals (shown in Fig. 6).

We also note that the galaxy masses and luminosities used in the simulations were on average lower than those examined in this work: the model galaxies in the simulations reached $M_* \approx 10^{10-11}$ M$_\odot$ at $z = 0$, whereas the galaxies in the DISC-LZ sample are within that stellar mass range by $0.5 \leq z \leq 2$ (Ilbert et al. 2009; Whitaker et al. 2011; Hartley et al. 2013). This makes a direct comparison between the simulations and this work more difficult, as bar fraction also depends on stellar mass (Sheth et al. 2008, 2012; Melvin et al. 2014). Kraljic et al. predict that massive disc galaxies will be more likely to form bars at higher redshift than lower mass disc galaxies due to higher mass galaxies reaching dynamical maturity at earlier epochs. This is qualitatively consistent with our finding that the bar fraction at $z \sim 2$ may be as high as 11 per cent within 1σ combined uncertainties (Section 2.5), but a direct and quantitative theoretical comparison to our observational result is currently not possible given available simulations. Expanded simulations encompassing galaxies with higher stellar masses would help to advance this field further.

Our results agree with previous work that the main epoch of disc settling (and thus bar formation) in the disc galaxy population begins at $z < 1$. However, bars are not completely absent even at $z \sim 2$: some discs at the masses probed by our sample ($10 \lesssim \log M_*[{\rm M}_\odot] \lesssim 11.3$) are mature enough even by this epoch (~ 3–4 Gyr after the big bang) to host a bar.

Whether the bar features are analogous to long-lived bars in dynamically cold discs at lower redshift or are shorter lived features triggered within dynamically warmer discs is unclear from examination of bar fractions alone. Examination of individual simulated galaxies by Kraljic et al. indicates that bars formed at $z > 1.5$ tend to undergo shorter cycles of formation and destruction, and there is some evidence that short-lived grand design spiral features

more commonly associated with mature discs can be triggered by interactions at $z > 2$ (Law et al. 2012a).

Thus, the incidence of bars in massive high-redshift discs may be due at least in part to galaxy interactions and mergers, combined with shorter bar lifetimes due to dynamically warmer discs. Minor galaxy mergers may dynamically heat a disc and destroy a bar, or they may trigger the formation of a bar, depending on the particulars of the interaction (Noguchi 1988; Gerin, Combes & Athanassoula 1990; Berentzen et al. 2003, 2004). The relative likelihood of these contrasting end results, combined with the incidence of minor mergers among this population at $z \lesssim 2$ (e.g. Lotz et al. 2011), may combine to produce a net effect that stabilizes the bar fraction at $f_{bar} \sim 10$ per cent during this epoch of galaxy assembly.

Among the galaxies in the highest redshift bin of the sample, two of the eight barred galaxies appear to be undergoing an interaction or merger, and another two appear tidally disturbed, possibly by a nearby companion. This may suggest these bar features are merger induced; on the other hand, mergers and interactions are not particularly rare during this epoch of galaxy assembly, so their appearance in the same galaxy population during the same epoch does not necessarily indicate a causal link.

To investigate this further, we examined the distributions of Galaxy Zoo vote fractions for the question 'Is the galaxy currently merging or is there any sign of tidal debris?', a second-tier question in the classification tree to which the possible responses are 'Merger', 'Tidal features', 'Both', or 'Neither'. Kolmogorov–Smirnov (KS) tests between the barred and unbarred disc galaxy samples in any redshift bin for vote fractions for responses f_{merger}, f_{tidal}, f_{both}, and the sum of these fractions, are inconclusive (typical $p \sim 0.4$, with $0.08 \leq p \leq 0.92$ among the KS tests, meaning the null hypothesis cannot be ruled out for any test). Resolving the question of whether shorter lived bars are triggered by interactions and/or mergers may be possible in the future, upon the full reduction of Galaxy Zoo: CANDELS data and the addition of galaxy images from the remaining CANDELS fields to the Galaxy Zoo sample.

4 SUMMARY

Using visual classifications of rest-frame optical *HST* galaxy images from the ongoing Galaxy Zoo: CANDELS project, we examined for the first time the fraction of disc galaxies hosting a bar feature to $z \sim 2$ in order to trace the dynamical state of discs as early as ~ 3 Gyr after the big bang. We find that the bar fraction to $z \sim 1$ is consistent with previous studies using similar analysis methods.

At $z > 1$, the bar fraction is approximately 10 per cent and consistent with no evolution to $z \sim 2$. This is qualitatively consistent with the predictions of zoom-in cosmological simulations, although further work is needed to determine whether simulations of disc galaxies with $L > L^*$ predict the same quantitative strong bar fraction at $z < 2$.

That the bar fraction from $0.5 < z < 2$ appears to be small but constant among massive disc galaxies implies that massive disc dynamics do not rapidly change on average over this period. Further clarification may come in the future when additional detailed morphological classifications of deep $z \sim 2$ rest-frame optical galaxy images are available. Future comparison with independent morphologies of the same galaxies (e.g. Kartaltepe et al. 2014) as well as additional simulations will help provide a more nuanced understanding of the underlying physical causes of this apparently stable bar fraction.

REFERENCES

Abraham R. G., Tanvir N. R., Santiago B. X., Ellis R. S., Glazebrook K., van den Bergh S., 1996, MNRAS, 279, L47
Abraham R. G., Merrifield M. R., Ellis R. S., Tanvir N. R., Brinchmann J., 1999, MNRAS, 308, 569
Aguerri J. A. L., Mndez-Abreu J., Corsini E. M., 2009, A&A, 495, 491
Athanassoula E., 2005, Celest. Mech. Dyn. Astron., 91, 9
Athanassoula E., Machado R. E. G., Rodionov S. A., 2013, MNRAS, 429, 1949
Balestra I. et al., 2010, A&A, 512, A12
Bamford S. P. et al., 2009, MNRAS, 393, 1324
Bennett C. L. et al., 2013, ApJS, 208, 20
Berentzen I., Athanassoula E., Heller C. H., Fricke K. J., 2003, MNRAS, 341, 343
Berentzen I., Athanassoula E., Heller C. H., Fricke K. J., 2004, MNRAS, 347, 220
Berentzen I., Shlosman I., Martinez-Valpuesta I., Heller C. H., 2007, ApJ, 666, 189200
Binney J., Merrifield M., 1998, Galactic astronomy. Princeton Univ Press, Princeton, NJ
Blanton M. R., Roweis S., 2007, AJ, 133, 734
Cameron E., 2011, PASA, 28, 128
Cameron E. et al., 2010, MNRAS, 409, 346
Cardamone C. N. et al., 2010, ApJS, 189, 270
Carilli C. L., Walter F., 2013, ARA&A, 51, 105
Casteels K. R. V. et al., 2013, MNRAS, 429, 1051
Cheung E. et al., 2013, ApJ, 779, 162
Cimatti A. et al., 2002, A&A, 392, 395
Cirasuolo M. et al., 2007, MNRAS, 380, 585
Clopper C. J., Pearson E. S., 1934, Biometrika, 26, 404
Combes F., 2009, in Jogee S., Marinova I., Hao L., Blanc G. A., eds, ASP Conf. Ser. Vol. 419, Galaxy Evolution: Emerging Insights and Future Challenges. Astron. Soc. Pac., San Francisco, p. 31
Conselice C. J., Bershady M. A., Dickinson M., Papovich C., 2003, AJ, 126, 1183
Dahlen T. et al., 2013, ApJ, 775, 93
Darg D. W. et al., 2010a, MNRAS, 401, 1043
Darg D. W. et al., 2010b, MNRAS, 401, 1552
Davis M. et al., 2007, ApJ, 660, L1

de Vaucouleurs G., de Vaucouleurs A., Corwin H. G., Jr Buta R. J., Paturel G., Fouqué P., 1991, Third Reference Catalogue of Bright Galaxies. Volume I: Explanations and references. Volume II: Data for galaxies between 0$^{>h}$ and 12^h. Volume III: Data for galaxies between 12^h and 24^h. Springer-Verlag, Berlin

Elmegreen B. G., Elmegreen D. M., 2005, ApJ, 627, 632

Elmegreen D. M., Elmegreen B. G., Hirst A. C., 2004a, ApJ, 604, L21

Elmegreen B. G., Elmegreen D. M., Hirst A. C., 2004b, ApJ, 612, 191

Elmegreen D. M., Elmegreen B. G., Ravindranath S., Coe D. A., 2007, ApJ, 658, 763

Emsellem E. et al., 2011, MNRAS, 414, 888

Fontana A. et al., 2014, A&A, in press

Förster Schreiber N. M. et al., 2009, ApJ, 706, 1364

Förster Schreiber N. M., Shapley A. E., Erb D. K., Genzel R., Steidel C. C., Bouché N., Cresci G., Davies R., 2011, ApJ, 731, 65

Friedli D., Benz W., 1993, A&A, 268, 6585

Galametz A. et al., 2013, ApJS, 206, 10

Gawiser E. et al., 2006, ApJS, 162, 1

Gehrels N., 1986, ApJ, 303, 336

Gerin M., Combes F., Athanassoula E., 1990, A&A, 230, 37

Giavalisco M. et al., 2004, ApJ, 600, L93

Grogin N. A. et al., 2011, ApJS, 197, 35

Guo Y. et al., 2013, ApJS, 207, 24

Hartley W. G. et al., 2013, MNRAS, 431, 3045

Häussler B. et al., 2007, ApJS, 172, 615

Ilbert O. et al., 2009, ApJ, 690, 1236

Jogee S. et al., 2004, ApJ, 615, L105

Kartaltepe J. S. et al., 2014, preprint (arXiv:1401.2455)

Kassin S. A. et al., 2012, ApJ, 758, 106

Koekemoer A. M. et al., 2007, ApJS, 172, 196

Koekemoer A. M. et al., 2011, ApJS, 197, 36

Kraljic K., Bournaud F., Martig M., 2012, ApJ, 757, 60 (K12)

Lambas D. G., Maddox S. J., Loveday J., 1992, MNRAS, 258, 404

Law D. R., Steidel C. C., Erb D. K., Larkin J. E., Pettini M., Shapley A. E., Wright S. A., 2009, ApJ, 697, 2057

Law D. R., Shapley A. E., Steidel C. C., Reddy N. A., Christensen C. R., Erb D. K., 2012a, Nature, 487, 338

Law D. R., Steidel C. C., Shapley A. E., Nagy S. R., Reddy N. A., Erb D. K., 2012b, ApJ, 745, 85

Lawrence A. et al., 2007, MNRAS, 379, 1599

Le Fèvre O. et al., 2004, A&A, 428, 1043

Lilly S. J. et al., 2007, ApJS, 172, 70

Lintott C. J. et al., 2008, MNRAS, 389, 1179

Lintott C. et al., 2011, MNRAS, 410, 166

Lotz J. M., Jonsson P., Cox T. J., Croton D., Primack J. R., Somerville R. S., Stewart K., 2011, ApJ, 742, 103

Lupton R., Blanton M. R., Fekete G., Hogg D. W., O'Mullane W., Szalay A., Wherry N., 2004, PASP, 116, 133

Marchesini D., Stefanon M., Brammer G. B., Whitaker K. E., 2012, ApJ, 748, 126

Masters K. L. et al., 2011, MNRAS, 411, 2026

Masters K. L. et al., 2012, MNRAS, 424, 2180

Melvin T. et al., 2014, MNRAS, 438, 2882

Moore B., Katz N., Lake G., Dressler A., Oemler A., 1996, Nat, 379, 613

Nair P. B., Abraham R. G., 2010, ApJ, 714, L260

Noguchi M., 1988, A&A, 203, 259

Odewahn S. C., 1996, in Buta R., Crocker D. A., Elmegreen B. G., eds, ASP Conf. Ser. Vol. 91, IAU Colloq. 157: Barred Galaxies. Astron. Soc. Pac., San Francisco, p. 30

Padilla N. D., Strauss M. A., 2008, MNRAS, 388, 1321

Scoville N. et al., 2007, ApJS, 172, 1

Sellwood J. A., 2013, in Oswalt T. D., Gilmore G., eds, Dynamics of Disks and Warps. Springer-Verlag, Berlin, p. 923

Sérsic J. L., 1968, Atlas de galaxias australes. Observatorio Astronomico, Cordoba, Argentina

Sheth K., Regan M. W., Scoville N. Z., Strubbe L. E., 2003, ApJ, 592, L13

Sheth K. et al., 2008, ApJ, 675, 1141

Sheth K., Melbourne J., Elmegreen D. M., Elmegreen B. G., Athanassoula E., Abraham R. G., Weiner B. J., 2012, ApJ, 758, 136

Simmons B. D., Urry C. M., 2008, ApJ, 683, 644

Simpson C. et al., 2012, MNRAS, 421, 3060

Simpson R. J. et al., 2013, preprint (arXiv:1301.5193)

Skibba R. A. et al., 2012, MNRAS, 423, 1485

Tacconi L. J. et al., 2010, Nature, 463, 781

Tacconi L. J. et al., 2013, ApJ, 768, 74

Taylor M. B., 2005, in Shopbell P., Britton M., Ebert R., eds, ASP Conf. Ser. Vol. 347, Astronomical Data Analysis Software and Systems XIV. Astron. Soc. Pac., San Francisco, p. 29

van der Wel A. et al., 2012, ApJS, 203, 24

Vanzella E. et al., 2008, A&A, 478, 83

Villa-Vargas J., Shlosman I., Heller C., 2010, ApJ, 719, 14701480

Whitaker K. E. et al., 2011, ApJ, 735, 86

Willett K. W. et al., 2013, MNRAS, 435, 2835

Wright E. L., 2006, PASP, 118, 1711

[1]*Oxford Astrophysics, Denys Wilkinson Building, Keble Road, Oxford OX1 3RH, UK*

[2]*Institute of Cosmology & Gravitation, University of Portsmouth, Dennis Sciama Building, Portsmouth PO1 3FX, UK*

[3]*Adler Planetarium, 1300 S. Lake Shore Drive, Chicago, IL 60605, USA*

[4]*SEPnet,¶ South East Physics Network, School of Physics & Astronomy, University of Southampton, Highfield, Southampton SO17 1BJ, UK*

[5]*School of Physics and Astronomy, University of Minnesota, 116 Church St SE, Minneapolis, MN 55455, USA*

[6]*Department of Physics and Astronomy, University of Alabama, Box 870324, Tuscaloosa, AL 35487, USA*

[7]*Department of Astronomy and Astrophysics, University of California, 1156 High Street, Santa Cruz, CA 95064, USA*

[8]*Institute for Astronomy, ETH Zürich, Wolfgang-Pauli-Strasse 27, CH-8093 Zürich, Switzerland*

[9]*National Optical Astronomy Observatory, 950 N. Cherry Ave, Tucson, AZ, 85719, USA*

[10]*Department of Astronomy, University of Michigan, Ann Arbor, MI 48104, USA*

[11]*Institut de Cincies del Cosmos. Universitat de Barcelona (UB-IEEC), Mart i Franqus 1, E-08028 Barcelona, Spain*

[12]*School of Physics & Astronomy, University of Nottingham, Nottingham NG7 2RD, UK*

[13]*Space Telescope Science Institute, 3700 San Martin Drive, Baltimore, MD 21218, USA*

[14]*Department of Physics and Astronomy, University of Kentucky, Lexington, KY 40506, USA*

[15]*Department of Physics and Astronomy, University of Missouri-Kansas City, 5110 Rockhill Road, Kansas City, MO 64110, USA*

[16]*Department of Physics and Astronomy & PITT PACC, University of Pittsburgh, Pittsburgh, PA 15217, USA*

[17]*UC Observatories/Lick Observatory and Department of Astronomy and Astrophysics, University of California, Santa Cruz, CA 95064, USA*

[18]*Department of Astronomy, The University of Texas at Austin, Austin, TX 78712, USA*

[19]*INAF-Osservatorio Astronomico di Roma, Via Frascati 33, I-00040 Monteporzio, Italy*

[20]*Centre for Astronomy and Astrophysics, University of Lisbon, P-1349-018 Lisbon, Portugal*

[21]*Centre for Astrophysics Research, University of Hertfordshire, College Lane, Hatfield AL10 9AB, UK*

[22]*Department of Physics and Astronomy, The Johns Hopkins University, Baltimore, MD 21218, USA*

[23]*Max-Planck-Institut für extraterrestrische Physik, Giessenbachstrasse 1, D-85748 Garching bei München, Germany*

[24]*European Southern Observatory/Joint ALMA Observatory, 3107 Alonso de Cordova, Vitacura 763-0355 Santiago, Chile*

This paper has been typeset from a TEX/LATEX file prepared by the author.